Deletion of Monoamine Oxidase A in a Prostate Cancer Model Enhances Anti-tumor Immunity Through Reduced Immune Suppression

Jessica A. Lapierre[a,b], Lauren A. Geary[a,b], Julie K. Jang[c], Alan L. Epstein[c], Frank Hong[a], Jean C. Shih[a,b,d,e,f,*]

[a]Department of Pharmacology and Pharmaceutical Sciences, School of Pharmacy, University of Southern California, 1985 Zonal Ave., Los Angeles, California, USA

[b]USC-Taiwan Center for Translational Research, University of Southern California, Los Angeles, California, USA

[c]Department of Pathology, Keck School of Medicine, University of Southern California, Los Angeles, California, USA

[d]Department of Cell and Neurobiology, Keck School of Medicine, University of Southern California, Los Angeles, California, USA

[e]Department of Integrative Anatomical Sciences, Keck School of Medicine, University of Southern California, Los Angeles, CA, USA

[f]Norris Comprehensive Cancer Center, Keck School of Medicine, University of Southern California, Los Angeles, CA, USA

Present address of J.A.L: Dicerna Pharmaceuticals, Inc., Lexington, MA, USA

Present address of F.H.: Bio-Synthesis, Inc., Lewisville, TX, USA

*Corresponding author: Jean C. Shih, Ph.D., Dept. of Pharmacology and Pharmaceutical Sciences, School of Pharmacy, University of Southern California, Rm. 518, 1985 Zonal Ave., Los Angeles, CA 90089. Tel.: 323-442-1441; E-mail: jcshih@usc.edu

Abbreviations

Arg1, Arginase 1; DKO, double knockout; DLP, dorsolateral prostate; HIF-1a, hypoxia-inducible factor 1-alpha; IFNγ, interferon gamma; iNOS, inducible nitric oxide synthase; MAO A, monoamine oxidase A; MDSC, myeloid-derived suppressor cell; Pten, phosphatase and tensin homolog

Declarations of competing interest

JCS is an inventor on the related patents concerning MAO inhibitor-based compounds for cancer treatment. All other authors have no competing interests to declare.

Ethics Committee Approval and Patient Consent

Not applicable.

Availability of data and materials

Data relevant to all study findings are presented in the paper.

CRediT authorship contribution statement

Conceptualization: JCS, LAG; Data curation: JAL, LAG, JKJ; Formal analysis: JAL, LAG; Funding acquisition: JCS, ALE; Investigation: JAL, LAG; Methodology: ALE, JAL, LAG, JKJ, JCS; Project administration: JCS; Resources: JCS; Software: LAG, JAL; Supervision: JCS; Validation: ALE, LAG, JCS; Visualization: JAL, LAG, JKJ; Roles/Writing - original draft: JCS, JAL, LAG; Writing - review & editing: JCS, FH, JAL.

Abstract

We have previously shown that monoamine oxidase A (MAO A) mediates prostate cancer growth and metastasis. Further, *MAO A/Pten* double knockout (DKO) mice were generated and demonstrated that the deletion of *MAO A* delayed prostate tumor development in the *Pten* knockout mouse model of prostate adenocarcinoma. Here, we investigated its effect on immune cells in the tumor microenvironment in *MAO A/Pten* DKO mouse model. Our results shows that Paraffin embedded prostate tissues from *MAO A/Pten* DKO mice had elevated markers of immune stimulation ($CD8^+$ cytotoxic T cells, granzyme B, and IFNγ) and decreased expression of markers of immune suppression (FoxP3, CD11b, HIF-1-alpha, and arginase 1) compared to parental *Pten* knockouts (*MAO A* wildtype). $CD11b^+$ myeloid derived suppressor cells (MDSC) were the primary immunosuppressive cell types in these tumors. The data suggest that deletion of *MAO A* reduces immune suppression in prostate tumors to enhance antitumor immunity in prostate cancer. Thus, *MAO A* inhibitor may alleviate immune suppression, increase the antitumor immune response and be used for cancer immunotherapy.

Keywords: prostate cancer, monoamine oxidase A, immune suppression, mouse model

1. Introduction

Monoamine oxidase (*MAO*) is a key enzyme regulating serotonin, norepinephrine, dopamine, and other neurotransmitters that mediate synaptic transmission to control brain functions. Monoamine oxidase A (*MAO A*) and B (*MAO B*) isoenzymes represent two distinct proteins with different physiological roles [1,2]. *MAO A* serves as a key determinant of aggression, depression, and autism, establishing the genetic basis of mental disorders [3,4]. *MAO B* plays a critical role in neurodegenerative diseases such as Parkinson's disease and Alzheimer's disease [5].

Intriguingly, *MAO A* is overexpressed in prostate tumors and increased further in higher-Gleason grade prostate tumors. *MAO A* inhibitors suppressed prostate tumor growth or bone metastasis in a mouse xenograft model, suggesting a potential role of *MAO A* in prostate cancer progression [6,7]. *MAO A* inhibitors showed efficacy against both androgen-sensitive and androgen-resistant prostate cancer cells *in vitro* [8]. *MAO A* was also overexpressed in classical Hodgkin lymphoma and *MAO A* inhibitors reduced its growth *in vitro* [9]. To target *MAO A* inhibitor specifically to cancer, near-infrared dye conjugated with a *MAO A* Inhibitor, clorgyline, was developed. Clorgyline is a specific *MAO A* inhibitor. NMI reduces prostate cancer growth more effectively than clorgyline and can be used for non-invasive diagnosis [10]. Decreasing *MAO A* activity by clorgyline or NMI reduced glioma progression in a mouse xenograft model, which showed increased macrophage infiltration in tumors [11]. NMI exhibited greater potency than previously FDA-approved drugs against brain, prostate, and non-small cell lung cancer cells *in vitro* [12]. The optimal dose and potential off-target organs of concern for NMI were determined via biodistribution imaging kinetics analysis [13]. These works led to a phase II clinical trial, which demonstrated the efficacy of the non-selective irreversible *MAO A* and *MAO B* inhibitor phenelzine in patients with biochemical recurrent castration sensitive prostate cancer [14]. The

roles of *MAO A* and *B* isoenzymes in cancer, brain and heart diseases, and many other functions have been reviewed recently [15,16].

The tumor microenvironment of solid tumors is a heterogeneous mixture of epithelial, mesenchymal, and immune cells. The types and functions of infiltrating cells present are highly variable and partially dependent on factors secreted by the tumor [17]. Analysis of immune cell infiltration can shed important light on the activated status of the immune response to the tumor (tumor immunogenicity) and the type of immunosuppression present at the time of biopsy.

Antitumor responses are mediated by natural killer cells, $CD8^+$ cytotoxic T cells, and M1 macrophages, which are promoted by Th1 differentiated $CD4^+$ helper T cells [18]. Despite the capability of antitumor immune cells to mount immune responses, tumors have a number of mechanisms to escape immune action [19]. Myeloid-derived suppressor cells (MDSCs) are a heterogeneous subset of innate immune cells which play a significant role in tumor immune tolerance. Identified by cell-surface expression of CD11b, these cells directly mediate T cell suppression as well as expand other immunosuppressive cells such as T regulatory cells (T regs) and M2 macrophages [20]. In cancers, these cells are often recruited to the tumor microenvironment and induce immune suppression by repressing the activity of cytotoxic T cells [21].

MAO A is a known regulator of hypoxia through the direct stabilization of the transcription factor HIF-1a [6]. *MAO A* may also modulate the immune system through regulation of HIF-1a. Although a number of studies have explored the causes of immune suppression in cancer in animal models [22], the potential of *MAO A* to modulate immune responses in a prostate cancer animal model had yet to be examined.

MAO A is overexpressed in prostate cancer and increases further in advanced-stage prostate cancer, which was shown to facilitate prostate tumorigenesis [23,24]. To further elucidate *MAO A*'s effect on prostate cancer development, a conditional gene knockout technique was used to introduce prostate-specific *MAO A* deficiency to a *Pten*-KO murine model mimicking human prostate cancer [25]. The selective loss of *Pten* expression in the prostate of the conditional *Pten*-null mouse leads to spontaneous development of hyperplasia, which is followed by prostatic intracellular neoplasia (PIN) at 2 months of age, and adenocarcinoma by 3-6 months [26,27]. The combined loss of *MAO A* and *Pten* expression in the prostate of *MAO A/Pten* DKO mice drastically curtailed the development of invasive adenocarcinoma despite the onset of PIN by 6 months of age, suggesting that *MAO A* inactivation significantly abrogates PIN to prostate cancer transition initiated by *Pten* loss [25]. This paper describes the mechanism through which *MAO A* inhibition reduces prostate cancer growth. We hypothesized that hypoxia may alter the tumor microenvironment through enzymes such as arginase 1, allowing for the inhibition or expansion of immune cells associated with immune suppression.

2. Methods

2.1 Animal studies

The generation of conditional *MAO A/Pten* DKO mice was previously described [25]. All mice utilized for these experiments were 9 months old with the exception of one *Pten* KO mouse (age: 6 months) which showed advanced tumor progression and was pathologically diagnosed at similar stage to *Pten* KO mice at 9 months of age.

To study the effects of *MAO A* on tumor growth, $2x10^5$ mouse glioma cells (GL-26) expressing renilla luciferase were subcutaneously injected in the syngeneic *MAO A* KO or wild-type C57 B/L male mice. Tumor size was determined 10 days after the tumor implantation by bioluminescence imaging.

Mice were maintained in a 12 h day/light cycle with access to water or food according to a protocol approved by the University of Southern California Institutional Animal Care and Use Committee. All procedures conducted involving mice were approved (#20308) by Institutional Animal Care and Use Committee at the University of Southern California.

2.2 Immunohistochemical analysis

Dorsolateral prostate tissues were collected from 9 months old wild-type, *MAO A* KO, *Pten* KO, and *MAO A/Pten* DKO mice and fixed in buffered zinc formalin. Tissues were paraffin embedded and cut to 5μm sections onto glass microscope slides. For immunohistochemistry (IHC), antigen retrieval was performed in 10 mM sodium citrate buffer, pH 6.0 for 15 minutes at 95° C. Tissues were blocked in 10% normal goat serum in PBS containing 0.3% Triton X-100, pH 7.6 for one hour at room temperature. Tissues were probed with antibodies at optimized dilutions overnight at 4° and washed with PBS, pH 7.6. Detection was performed using appropriate IgG secondary antibody for 30 minutes at room temperature, followed by ABC reagent and DAB substrate. Tissues were counterstained and visualized by light microscopy.

Multiple antigen staining using Vector Blue© and Vector Red© (Vector Labs) chromogen substrates was performed as recommended by the manufacturer. Tissues used for multiple antigen staining were counterstained with Methyl Green (Vector Labs) and visualized by light microscopy. The following primary antibodies were used: anti-F4/80 (3H2113, Santa Cruz Biotechnology),

anti-granzyme B (2C5, Santa Cruz Biotechnology), anti-IFNγ (XMG1.2, BioLegend), anti-HIF-1a (241808, R&D Systems), anti-CD8 (H35, in-house), anti-CD11b (5C6, in-house), anti-arginase 1 (19/Arginase 1, BD Biosciences), anti-iNOS (polyclonal, Abcam), anti-FoxP3 (polyclonal, Abcam).

2.3 Statistical analysis

Representative images were taken from each animal group (n=3 mice per group, 3-5 high powered fields per mouse). All data are presented as mean ± SD. Differences between multiple groups were analyzed by one-way ANOVA followed by Tukey test to compare groups. Differences between two groups were analyzed by an independent t-test. P values of <0.05 were considered to be statistically significant. ImageJ software was used for the quantification of images.

3. Results

3.1 Tumor growth

To assess the potential impact of *MAO A*, tumor cells were implanted in *MAO A* KO mice and the tumor growth was monitored. GL-26 mouse glioma cells stably expressing renilla luciferase were subcutaneously implanted in syngeneic *MAO A* KO or wild-type C57 B/L male mice. After 10 days, tumor size was determined via bioluminescence imaging. Tumor growth was significantly reduced in *MAO A* KO mice when compared to wild-type mice (Figure 1). Even greater growth suppression was observed after similarly implanting in *MAO A/B* DKO mice (data not shown). We previously described the isolation of *MAO A/B* DKO mice, which exhibit biochemical and behavioral phenotypes that are more severe than either *MAO A* or *MAO B* KO mice [28].

Figure 1

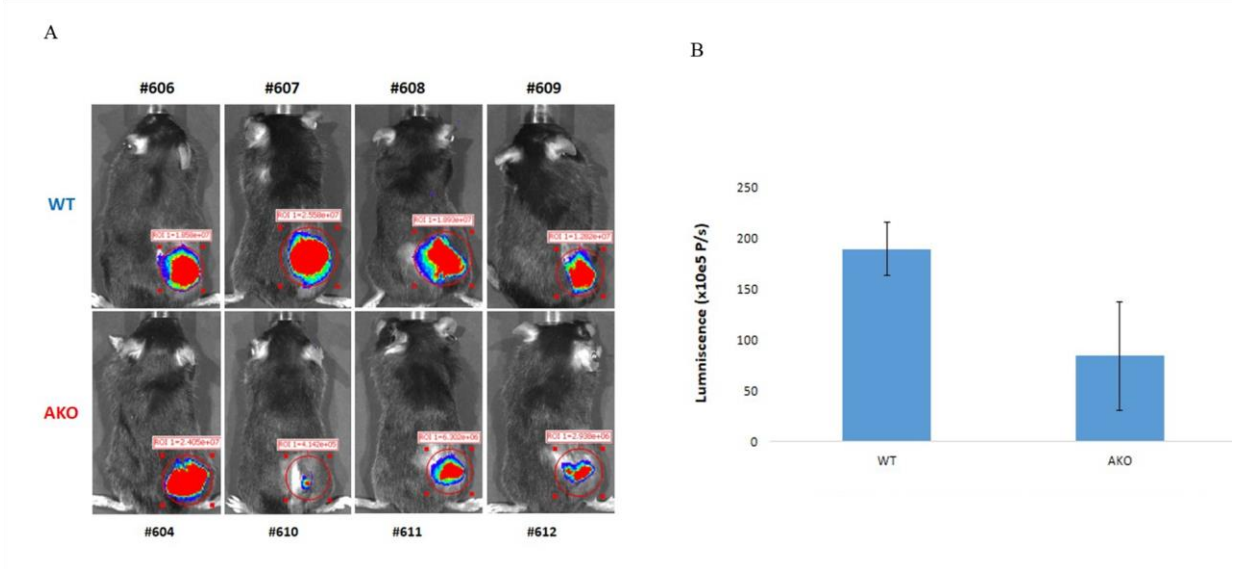

Figure 1

***MAO A* KO mice display reduced tumor growth.**

A. Subcutaneous GL26 tumor formation in wild type (WT) and *MAO A* KO (AKO) mice at 10 days post implantation. GL-26 mouse glioma cells (2 x 10^5/mouse) stably expressing renilla luciferase were subcutaneously injected in syngeneic *MAO A* KO or wild-type C57 B/L male mice. After 10 days, animals were imaged. Tumor size was determined by bioluminescence imaging. **B.** Comparison of subcutaneous GL26 mouse glioma tumors 10 days post tumor cell implantation. The bioluminescence signal intensity in syngeneic *MAO A* KO or wild-type C57 B/L male mice is shown.

3.2 *MAO A/Pten* DKO decreases recruitment of immune suppressive cells

In the spontaneously forming tumor model of *Pten* KO mice, introducing prostate-specific *MAO A* deficiency through conditional gene knockout significantly decreased the incidence of invasive

cancer [25]. To investigate the effects of deleting *MAO A* within the *Pten* knockout prostate cancer mouse model on the anti-tumor immune response, immunohistochemistry was performed using markers for $CD8^+$ cytotoxic T cells, $F4/80^+$ macrophages, $FoxP3^+$ T regulatory cells, and $CD11b^+$ myeloid-derived suppressor cells. Figure 2A shows a comparison of wild type, *MAO A* KO, *Pten* KO, and *MAO A/Pten* DKO dorsolateral mouse prostate tissues. *MAO A/Pten* DKO prostate tissue showed higher positive staining for CD8 than single *Pten* knockout with 52% more $CD8^+$ cells ($P<0.005$), whereas there was no significant difference in F4/80 positive staining between the two groups ($P=0.93$) (Figure 2B). Little to no positive staining for both antibodies were seen in the wild type or MAO A KO tissues. Alternatively, positive staining for immune suppressive cell markers, FoxP3 and CD11b, were markedly decreased in the *MAO A/Pten* DKO compared to the *Pten* KO. *MAO A/Pten* DKO prostate tissue showed decreases of 45% and 78% in the number of $FoxP3^+$ T regulatory cells and $CD11b^+$ MDSCs, respectively, as compared to the *Pten* KO ($P=0.008$, $P<0.005$).

Figure 2

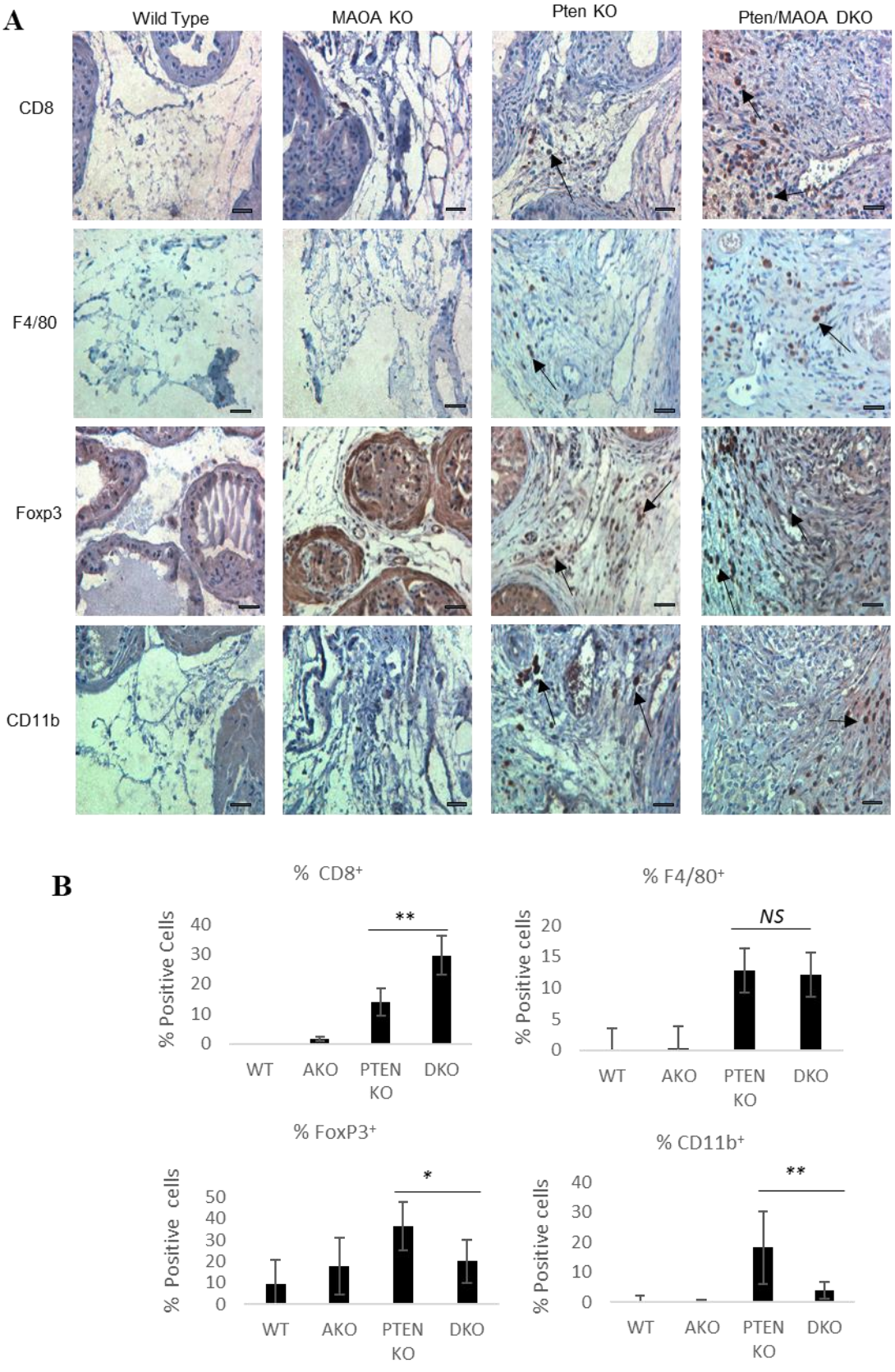
A
Wild Type
MAOA KO
Pten KO
Pten/MAOA DKO
CD8
F4/80
Foxp3
CD11b
B
% CD8+
% Positive Cells
40
30
20
10
0
**
WT
AKO
PTEN KO
DKO
% F4/80+
% Positive cells
20
15
10
5
0
NS
% FoxP3+
% Positive cells
50
40
30
20
10
0
*
% CD11b+
% Positive cells
40
30
20
10
0
**

Figure 2.

Representative IHC images of tissue sections from prostates of mice derived from the conditional *Pten* knockout model of mouse prostate adenocarcinoma.

A. Four genotypes described as wildtype (*Pten*$^{flox/flox}$; *MAOA*^{flox}), *MAOA* knockout (AKO; *Cre*$^{+/+}$; *Pten*$^{+/+}$; *MAOA*^{flox}), *Pten* KO (*Cre*$^{+/+}$; *Pten*$^{flox/flox}$; *MAOA*$^{+}$), and *Pten/MAOA* double knockout (DKO; *Cre*$^{+/+}$; *Pten*$^{flox/flox}$; *MAOA*^{flox}) were examined for the protein expression levels of the immune cell markers CD8, F4/80, FoxP3, and CD11b. Arrows point to positively staining leukocytes. Dorsolateral prostate lobe was examined for all four genotypes in n=3 mice per genotype at 9 months of age. Images at 400x magnification. Bar, 100 μm. **B.** Percent positive staining was quantified from number of nucleated positive cells per total nucleated stromal cells. * P<0.05; ** P<0.005; *NS, Not significant*

3.3 *MAO A/Pten* DKO shows a reduction in arginase 1 and iNOS stimulated immune suppressive cells in the tumor microenvironment

Immune suppressive cells in the tumor microenvironment from the heterogeneous population of myeloid lineage cells, such as MDSC, suppress T cell immune response and, thus, in the context of cancer, allow tumor progression through elevated production of two L-arginine-consuming enzymes—inducible nitric oxide synthase (iNOS, NOS2) and arginase 1 (Arg1). Under hypoxic conditions, MDSCs produce elevated levels of iNOS and Arg1, which prevent T cell division and activation by production of nitric oxide and inhibition of T cell receptor expression and antigen-specific T cell responses, respectively [29]. The *MAO A/Pten* DKO prostate tumor tissues showed a 74% reduction in iNOS^{+} staining as compared to the *Pten* KO indicating a less

immunosuppressive environment (P<0.005) (Figure 3). Arg1 was also decreased by 51% in *MAO A/Pten* DKO prostate tumors compared to *Pten* KO (P=0.002).

Figure 3

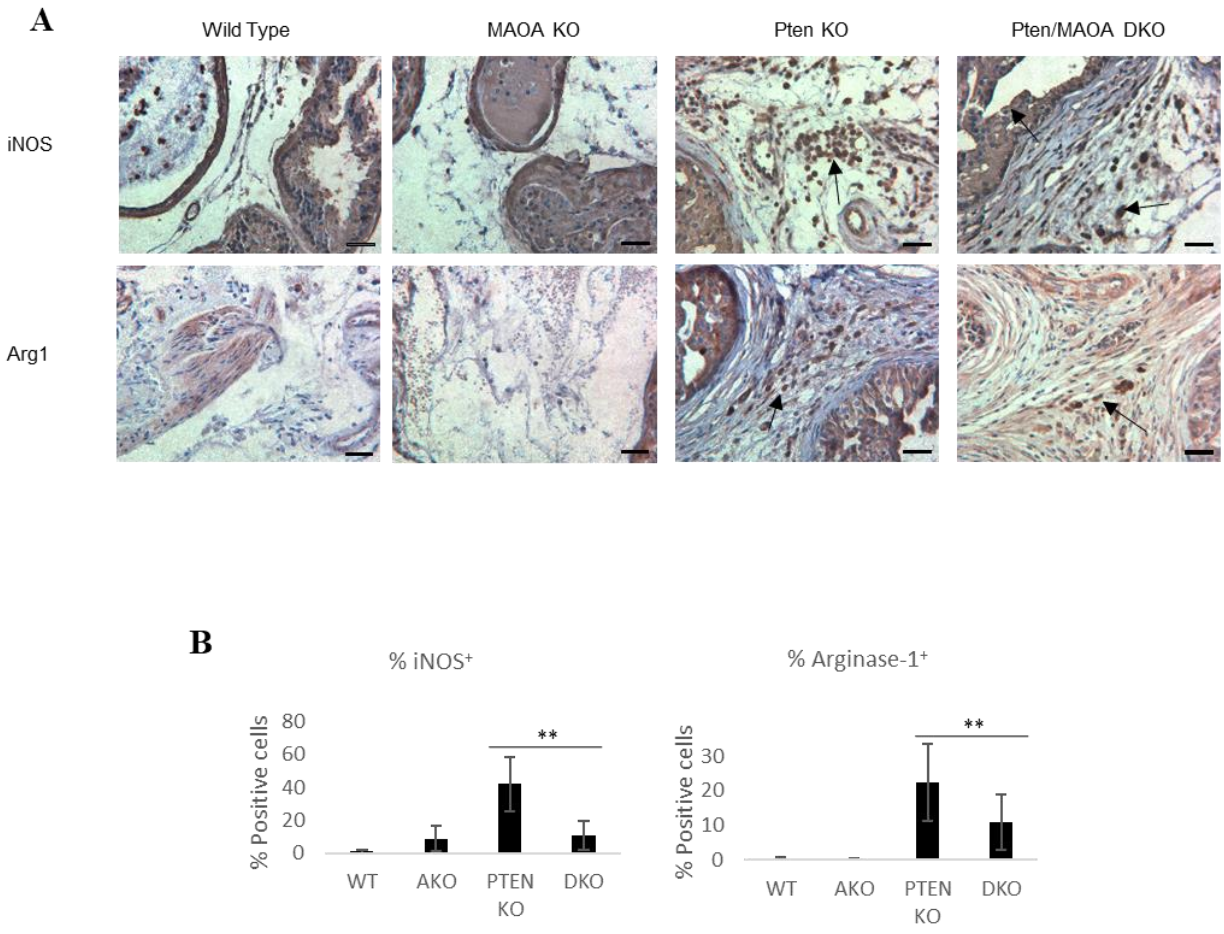

Figure 3.

Representative IHC images of tissue sections from prostates of mice derived from the conditional *Pten* knockout model of mouse prostate adenocarcinoma.

A. Four genotypes described as wildtype (*Pten*$^{flox/flox}$; *MAOA*^{flox}), *MAOA* knockout (AKO; *Cre*$^{+/+}$; *Pten*$^{+/+}$; *MAOA*^{flox}), *Pten* KO (*Cre*$^{+/+}$; *Pten*$^{flox/flox}$; *MAOA*$^{+}$), and *Pten/MAOA* double knockout (DKO; *Cre*$^{+/+}$; *Pten*$^{flox/flox}$; *MAOA*^{flox}) were examined for the protein expression levels of immune suppressed environment markers iNOS and Arginase-1. Arrows point to positively staining leukocytes. Dorsolateral prostate lobe was examined for all four genotypes in n=3 mice per genotype at 9 months of age. Images at 400x magnification. Bar, 100 μm. **B**. Percent positive staining was quantified from number of nucleated positive cells per total nucleated stromal cells. * P<0.05; ** P<0.005; *NS, Not significant*

To characterize the immune cells present in the tumor microenvironment as pro-tumorigenic (MDSCs, M2 macrophages) or anti-tumorigenic (M1 macrophages), multiple antigen staining was utilized to co-localize markers of monocytes with iNOS or Arg1. Based upon recent studies in colon cancer, F4/80^{+} Arg1^{+} cells were interpreted as indicative of "M2" macrophages and F4/80^{+} iNOS^{+} cells as indicative of "M1" macrophages [30]. Although iNOS is generally used as a marker for immune suppression, F4/80^{+}iNOS^{+} cells are characterized as having M1 phenotype. In this context, iNOS+ cells are no longer considered to be suppressive. The presence of polarized F4/80^{+} macrophages present in the *MAO A/Pten* DKO, compared to the *Pten* KO prostate cancer model, was determined by immunohistochemistry staining F4/80^{+} cells with Vector Blue© (Burlingame, CA) and either iNOS^{+} for M1 or Arg1^{+} for M2 polarized cells with Vector Red© (Burlingame, CA) (Figure 4A). Co-localization was seen in purple by histological observation. Our results show that there were 30% more F4/80^{+} iNOS^{+} "M1" macrophages in *MAO A/Pten* DKO than in *Pten* KO mouse prostate tumor tissues (P<0.05), but there was no significant

observable difference in F4/80$^+$ Arg1$^+$ "M2" macrophages (P>0.05) (Figure 4B). We observed more cells expressing the F4/80$^+$ iNOS$^+$ phenotype in the *MAO A/Pten* DKO mouse prostate tumor tissue than in the *Pten* KO; however, the difference in total iNOS$^+$ cells between *Pten* KO and *MAO A/Pten* DKO suggest a difference in iNOS producing myeloid cells other than F4/80$^+$ macrophages within the tumor microenvironment.

Multiple antigen staining was used to assess levels of iNOS and Arg1 co-expressed with CD11b$^+$ MDSCs in the *Pten* KO and *MAO A/Pten* DKO mouse prostate tissues and whether their presence contributed significantly more iNOS in the tumor microenvironment in the tumors of the *Pten* KO mouse prostate compared to the DKO. MDSC presence in the *Pten* KO versus the *MAO A*/*Pten* DKO was visualized by staining with Vector Blue© (Burlingame, CA) and staining for either iNOS$^+$ or Arg1$^+$ cells with Vector Red© (Burlingame, CA) (Figure 4A). A decreased presence of CD11b$^+$ iNOS$^+$ cells was observed in the *MAO A/Pten* DKO compared to the *Pten* KO (P<0.05); (Figure 4B).

Figure 4

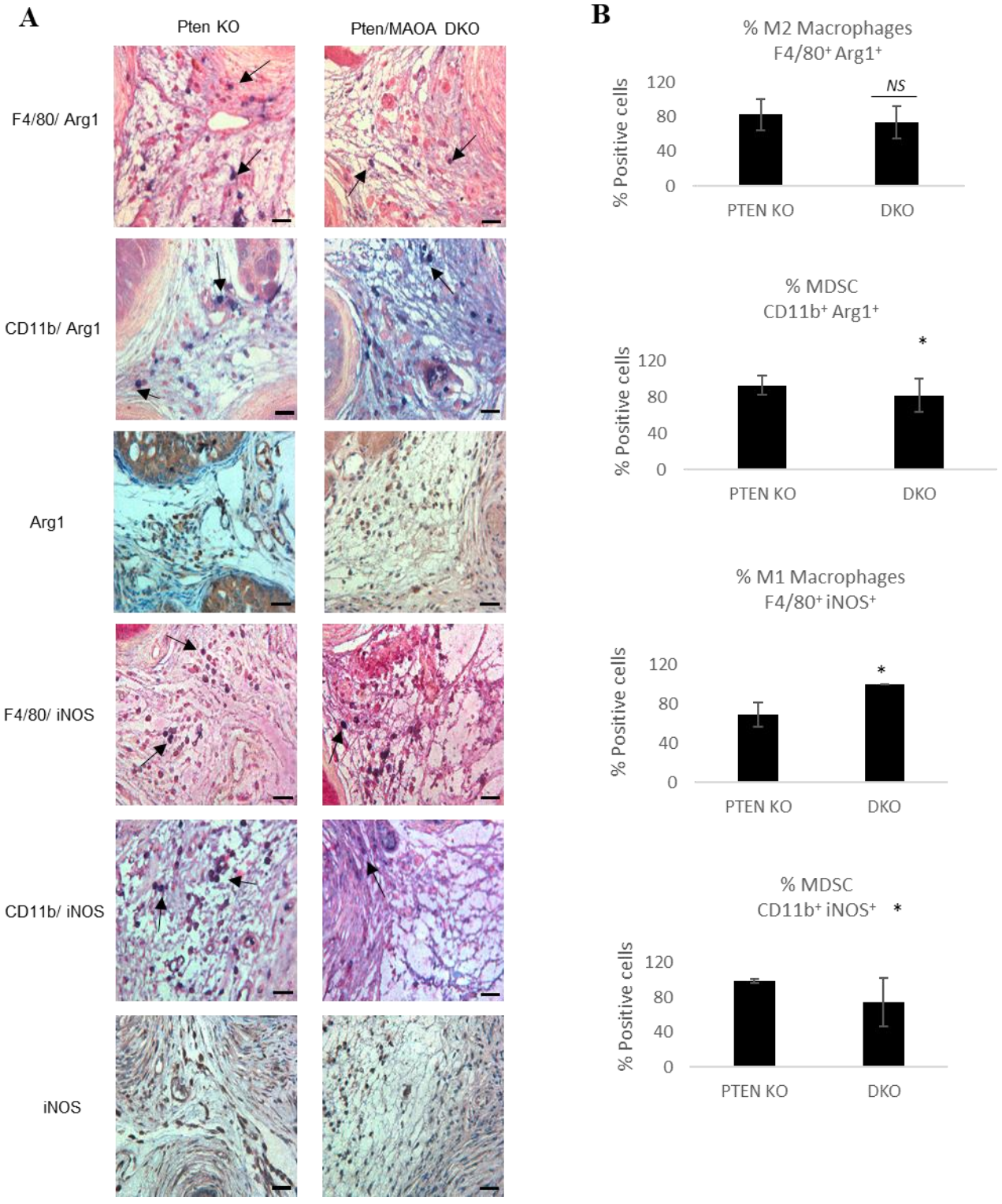
A
Pten KO
Pten/MAOA DKO
F4/80/ Arg1
CD11b/ Arg1
Arg1
F4/80/ iNOS
CD11b/ iNOS
iNOS
B
% M2 Macrophages
F4/80+ Arg1+
NS
% Positive cells
120
80
40
0
PTEN KO
DKO
% MDSC
CD11b+ Arg1+
*
% M1 Macrophages
F4/80+ iNOS+
% MDSC
CD11b+ iNOS+ *

Figure 4.

Representative IHC images of tissue sections from prostates of mice derived from the conditional *Pten* knockout model of mouse prostate adenocarcinoma.

A. The genotypes of interest described as *Pten* KO (*Cre*$^{+/+}$; *Pten*$^{flox/flox}$; *MAOA*$^{+}$) and *Pten/MAOA* double knockout (DKO; *Cre*$^{+/+}$; *Pten*$^{flox/flox}$; *MAOA*^{flox}) were examined for the co-localization of protein expression of the immune environment markers iNOS and Arginase-1 and markers for the immune cells which are producing them, F4/80 and CD11B. Arrows point to purple, double positive staining leukocytes. Dorsolateral prostate lobe was examined for both genotypes with n=3 mice per genotype at 9 months of age. Images at 400x magnification. Bar, 100 μm. **B.** Percent positive staining was quantified from the number of nucleated iNOS/Arg1 and F4/80/CD11B double positive cells per total number of nucleated immune cells. * P<0.05; ** P<0.005; *NS, Not significant*

3.4 Reduced HIF-1a and elevated granzyme B and IFNγ are found in *MAO A/Pten* DKO prostate tumors

To understand the mechanisms of reduced immune suppression in the *MAO A/Pten* DKO mice, we examined tissues for markers of immune activation. Immunohistochemistry revealed both granzyme B and IFNγ to be higher in the *MAO A/Pten* DKO mouse prostate tissues than the *Pten* KO with differences of 64% and 66% respectively (P<0.005) (Figure 5B). Both of these markers are implicated in T cell proliferation and cytotoxic function. Conversely, HIF-1a, a master regulator of hypoxia, was 76% higher in the *Pten* KO than the DKO as seen in Figure 5B

(P<0.005). This is consistent with published mechanisms of MDSC mediated immune suppression [31,32].

Figure 5

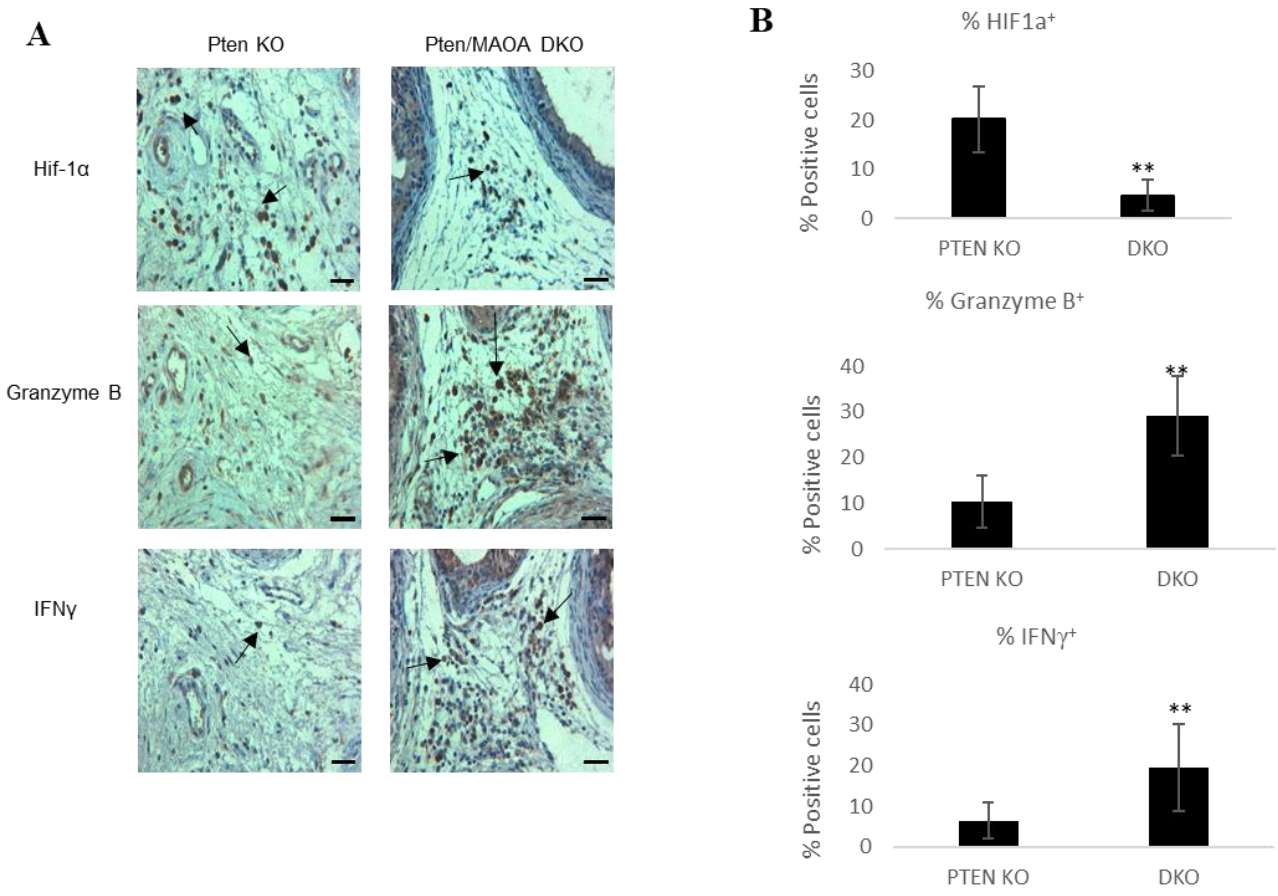

Figure 5.

Representative IHC images of tissue sections from prostates of mice derived from the conditional *Pten* knockout model of mouse prostate adenocarcinoma.

A. The two genotypes of interest described as *Pten* KO ($Cre^{+/+}$; $Pten^{flox/flox}$; $MAOA^{+}$), and *Pten/MAOA* double knockout (DKO; $Cre^{+/+}$; $Pten^{flox/flox}$; $MAOA^{flox}$) were examined for the protein expression levels of mechanistic immune response factors HIF-1a, granzyme B, and IFNγ. Arrows

point to positively staining leukocytes. Dorsolateral prostate lobe was examined for all four genotypes in n=3 mice per genotype at 9 months of age. Images at 400x magnification. Bar, 100 μm. **B.** Percent positive staining was quantified from number of nucleated positive cells per total nucleated stromal cells. * P<0.05; ** P<0.005; *NS, Not significant*

4. Discussion

Our data suggest that knocking out *MAO A* in the context of prostate cancer, at least within the conditional *Pten* KO mouse model of prostate adenocarcinoma, alters the immune system leading to an enhanced antitumor response. Specifically, the *MAO A/Pten* DKO showed higher positive staining for the recruitment of $CD8^+$ cytotoxic T cells into the tumor microenvironment. Coinciding with these results, we observed that the *MAO A/Pten* DKO prostate tumor tissues displayed less immune suppression based on the reduced positive staining for immunosuppressive cells, such as $FoxP3^+$ T regulatory cells and $CD11b^+$ myeloid-derived suppressor cells. Though also expressed in healthy prostatic epithelium, patients with prostate cancer have higher levels of $FoxP3^+$ T regulatory cells and dysfunctional $CD8^+$ cytotoxic T cells which are associated with a poorer prognosis [33]. In addition, the DKO mouse tissues also displayed less positive staining for two markers of an immune suppressed environment: iNOS and arginase 1. These findings support the hypothesis that knocking out *MAO A* can enhance the antitumor response of the immune system through the reduction of immune suppression allowing for cytotoxic T cell proliferation and targeting of the tumor cells.

While cellular expression of the F4/80 cell surface marker is heterogeneous, the overwhelming majority of such cells have been found to be macrophages [34]. and there was no

observed difference in these cells between the two groups. Interestingly, F4/80$^+$ macrophages have only a slight, non-significant reduction in the *Pten/MAO A* DKO compared to *Pten* KO. Of these, F4/80/iNOS double positive cells are significantly higher in *Pten/MA OA* DKO compared to *Pten* KO prostate tumors, possibly indicating enhanced M1 macrophage presence, and F4/80/Arg1 double positive cells (indicative of M2 macrophages) are slightly, but not significantly, decreased in the DKO compared to *Pten* KO. In contrast, double stains of iNOS and Arg1 with CD11b reveal that CD11b/iNOS and CD11b/Arg1 double positive cells are reduced in *Pten/MAO A* DKO tumors compared to *Pten* KO. These findings are consistent with our results from single stains of these markers, and indicate that iNOS and Arg1 producing CD11b$^+$ myeloid-derived cells, or MDSCs, are reduced in *MAO A/Pten* DKO tumors compared to *Pten* KO tumors. Garcia et al. recently found evidence of high levels of iNOS and Arg1 leading to expansion of MDSCs in the *Pten* null mouse prostate cancer model [35].

Upon further scrutiny, the observed reduction of immune suppression in the DKO prostate tumors can possibly be explained by evidence from the monocyte double stains. Our data showed that the *MAO A/Pten* DKO possessed more F4/80$^+$ iNOS$^+$ M1 macrophages than the *Pten* KO. Upon examination of total iNOS$^+$ in both groups, other myeloid cells contributed to the total production of iNOS and immune suppression. CD11b/iNOS double stains in the *Pten* KO and *MAO A/Pten* DKO mouse prostate tissues confirmed that MDSC are significant contributors to total iNOS$^+$ found in tumor tissues. Less CD11b$^+$ iNOS$^+$ MDSCs were seen in the DKO than the *Pten* KO. Additionally, the F4/80$^+$ and CD11b$^+$ double stains with Arg1 both showed no statistical difference between the single and DKO tissues examined. Overall, this suggests the importance of iNOS in this model of immune suppression mediated by *MAO A* and that the cells contributing to immune suppression via expression of iNOS in the *Pten* knockout are most probably MDSC. It

follows that the mechanism of reduced immune suppression in the DKO model comes from a reduction of iNOS+ MDSC, rather than reprogramming of macrophages towards an M2 phenotype.

Examination of markers indicating active immune processes allowed for further comprehension of the pathways being utilized by the immune cells within these tumors. The elevated levels of granzyme B in the *MAO A/Pten* DKO indicates restoration of functional cytotoxic T cell activity in tumors of these mice [36]. IFNγ's role in tumor immunity is multifaceted, participating in inhibition of tumor cells proliferation, activation of innate and adaptive immune response, and inhibition of angiogenesis [37]. In addition, Doedens et al. showed that loss of HIF-1a in myeloid cells relieved hypoxia-induced suppression of T cell activation through myeloid-derived iNOS and Arg1 [31]. The higher levels of granzyme B and IFNγ in combination with reduced HIF-1a support the hypothesis that reduced immune suppression in the *MAO A/Pten* DKO mice may be due to reduced hypoxic stress.

In conclusion, these studies demonstrate a role for *MAO A* in HIF-1a induction of immune suppressor cells in prostate tumors. The deletion of *MAO A* reduces immune suppression in prostate tumors to enhance antitumor immunity in prostate cancer. These findings explain why subcutaneously implanted GL26 mouse glioma cells showed significantly reduced tumor growth in *MAO A* KO mice than wild-type mice (Figure 1). Taken together, our results show that MAO A inhibitor may alleviate immune suppression, enhance the antitumor immune response and be used as a cancer immunotherapy agent. Further studies to clarify the manner in which *MAO A* modulates immune response are needed. Potential pathways to consider involve the direct and indirect downstream effects of knocking out *MAO A*. One approach would be to study whether the observed immune modulation is induced by elevated levels of serotonin. Accumulated evidence

suggests that serotonin facilitates Th1 differentiation of $CD4^+$ T cells, and previous studies showing that physiological doses of serotonin induce the secretion of Th1 cytokines such as IL-1β, IFN-γ, and IL-12 [38]. In addition, future investigation into global immune system changes independent of the tumor microenvironment as a result of knocking out *MAO A* would also be of interest.

Acknowledgments

This work was supported by the U.S. Department of Defense Prostate Cancer Research Program grant W81xWH-12-1-0282, Daniel Tsai Family Fund, and Boyd and Elsie Welin Professorship to J. C. Shih. Julie K. Jang is a TL1 Trainee awarded through Southern California Clinical and Translational Science Institute at the University of Southern California, Keck School of Medicine (NIH Grant Award Number TL1TR000132). National Cancer Institute Cancer Center Shared Grant award P30CA014089 provided additional funding.

References

1. A.W. Bach, N.C. Lan, D.L. Johnson, C.W. Abell, M.E. Bembenek, S.W. Kwan, P.H. Seeburg, J.C. Shih. cDNA cloning of human liver monoamine oxidase A and B: molecular basis of differences in enzymatic properties. Proc. Natl. Acad. Sci. USA. 85 (1988) 4934-4938. DOI: 10.1073/pnas.85.13.4934.

2. J.C. Shih, K. Chen, M.J. Ridd. Monoamine oxidase: from genes to behavior. Annu. Rev. Neurosci. 22 (1999) 197-217. DOI: 10.1146/annurev.neuro.22.1.197.

3. O. Cases, I. Seif, J. Grimsby, P. Gaspar, K. Chen, S. Pournin, U. Müller, M. Aguet, C. Babinet, J.C. Shih, E. De Maeyer. Aggressive behavior and altered amounts of brain serotonin and norepinephrine in mice lacking MAOA. Science. 268 (1995) 1763-1766. DOI: 10.1126/science.7792602.

4. M. Bortolato, S.C. Godar, L. Alzghoul, J. Zhang, R.D. Darling, K.L. Simpson, V. Bini, K. Chen, C.L. Wellman, R.C. Lin, J.C. Shih. Monoamine oxidase A and A/B knockout mice display autistic-like features. Int. J. Neuropsychopharmacol. 16 (2013) 869-888. DOI: 10.1017/S1461145712000715.

5. M. Bortolato, K. Chen, J.C. Shih. Monoamine oxidase inactivation: from pathophysiology to therapeutics. Adv. Drug Deliv. Rev. 60 (2008) 1527-1533. DOI: 10.1016/j.addr.2008.06.002

6. J.B. Wu, C. Shao, X. Li, Q. Li, P. Hu, C. Shi, Y. Li, Y.T. Chen, F. Yin, C.P. Liao, B.L. Stiles, H.E. Zhau, J.C. Shih, L.W. Chung. Monoamine oxidase A mediates prostate tumorigenesis and cancer metastasis. J. Clin. Invest. 124 (2014) 2891-2908. DOI: 10.1172/JCI70982.

7. J.B. Wu, L. Yin, C. Shi, Q. Li, P. Duan, J.M. Huang, C. Liu, F. Wang, M. Lewis, Y. Wang, T.P. Lin, C.C. Pan, E.M. Posadas, H.E. Zhau, L.W.K. Chung. MAOA-dependent activation of Shh-

IL6-RANKL signaling network promotes prostate cancer metastasis by engaging tumor-stromal cell interactions. Cancer Cell. 31 (2017) 368-382. DOI: 10.1016/j.ccell.2017.02.003.

8. S. Gaur, M.E. Gross, C.P. Liao, B. Qian, J.C. Shih. Effect of monoamine oxidase A (MAOA) inhibitors on androgen-sensitive and castration-resistant prostate cancer cells. Prostate. 79 (2019) 667-677. DOI: 10.1002/pros.23774.
9. P.C. Li, I.N. Siddiqi, A. Mottok, E.Y. Loo, C.H. Wu, W. Cozen, C. Steidl, J.C. Shih. Monoamine oxidase A is highly expressed in classical Hodgkin lymphoma. J. Pathol. 243 (2017) 220-229. DOI: 10.1002/path.4944.
10. J.B. Wu, T.P. Lin, J.D. Gallagher, S. Kushal, L.W. Chung, H.E. Zhau, B.Z. Olenyuk, J.C. Shih. Monoamine oxidase A inhibitor-near-infrared dye conjugate reduces prostate tumor growth. J. Am. Chem. Soc. 137 (2015) 2366-2374. DOI: 10.1021/ja512613j.
11. S. Kushal, W. Wang, V.P. Vaikari, R. Kota, K. Chen, T.S. Yeh, N. Jhaveri, S.L. Groshen, B.Z. Olenyuk, T.C. Chen, F.M. Hofman, J.C. Shih. Monoamine oxidase A (MAO A) inhibitors decrease glioma progression. Oncotarget. 7 (2016) 13842-13853. DOI: 10.18632/oncotarget.7283.
12. Q. Feng, Y. Lian, Y. Qian, J.C. Shih. Near-infrared MAO A inhibitor (NMI) outperformed FDA-approved chemotherapeutic agents in brain and other cancers: a bioinformatic analysis of NCI60 screening data. Brain Sci. 11 (2021) 1318. DOI: 10.3390/brainsci11101318.
13. R.W. Irwin, A.R. Escobedo, J.C. Shih. Near-infrared monoamine oxidase inhibitor biodistribution in a glioma mouse model. Pharm. Res. 38 (2021) 461-471. DOI: 10.1007/s11095-021-03012-0.

14. M.E. Gross, D.B. Agus, T.B. Dorff, J.K. Pinski, D.I. Quinn, O. Castellanos, P. Gilmore, J.C. Shih. Phase 2 trial of monoamine oxidase inhibitor phenelzine in biochemical recurrent prostate cancer. Prostate Cancer Prostatic Dis. 24 (2021) 61-68. DOI: 10.1038/s41391-020-0211-9.

15. J.C. Shih, P. Riederer, W. Maruyama, M. Naoi. Introduction to the special issue on monoamine oxidase A and B: eternally enigmatic isoenzymes. J. Neural Transm. (Vienna). 125 (2018) 1517-1518. DOI: 10.1007/s00702-018-1920-2.

16. J.C. Shih. Monoamine oxidase isoenzymes: genes, functions and targets for behavior and cancer therapy. J. Neural Transm. (Vienna). 125 (2018) 1553-1566. DOI: 10.1007/s00702-018-1927-8.

17. G.P. Dunn, L.J. Old, R.D. Schreiber. The immunobiology of cancer immunosurveillance and immunoediting. Immunity 21 (2004) 137-148. DOI: 10.1016/j.immuni.2004.07.017.

18. V. Appay, J.J. Zaunders, L. Papagno, J. Sutton, A. Jaramillo, A. Waters, P. Easterbrook, P. Grey, D. Smith, A.J. McMichael, D.A. Cooper, S.L. Rowland-Jones, A.D. Kelleher. Characterization of CD4(+) CTLs ex vivo. J. Immunol 168 (2002) 5954-5958. DOI: 10.4049/jimmunol.168.11.5954.

19. R.E. Sadun, S.M. Sachsman, X. Chen, K.W. Christenson, W.Z. Morris, P. Hu, A.L. Epstein. Immune signatures of murine and human cancers reveal unique mechanisms of tumor escape and new targets for cancer immunotherapy. Clin. Cancer Res. 13 (2007) 4016-4025. DOI: 10.1158/1078-0432.CCR-07-0016

20. M.G. Lechner, D.J. Liebertz, A.L. Epstein. Characterization of cytokine-induced myeloid-derived suppressor cells from normal human peripheral blood mononuclear cells. J. Immunol. 185 (2010) 2273-2284. DOI: 10.4049/jimmunol.1000901

21. M. Johansson, D.G. Denardo, L.M. Coussens. Polarized immune responses differentially regulate cancer development. Immunol. Rev. 222 (2008) 145-154. DOI: 10.1111/j.1600-065X.2008.00600.x

22. D. Lindner. Animal models and the tumor microenvironment: studies of tumor-host symbiosis. Semin. Oncol. 41 (2014) 146-155. DOI: 10.1053/j.seminoncol.2014.02.004

23. L. True, I. Coleman, S. Hawley, C.Y. Huang, D. Gifford, R. Coleman, T.M. Beer, E. Gelmann, M. Datta, E. Mostaghel, B. Knudsen, P. Lange, R. Vessella, D. Lin, L. Hood, P.S. Nelson. A molecular correlate to the Gleason grading system for prostate adenocarcinoma. Proc. Natl. Acad. Sci. USA. 103 (2006) 10991–10996. DOI: 10.1073/pnas.0603678103

24. D.M. Peehl, M. Coram, H. Khine, S. Reese, R. Nolley, H. Zhao. The significance of monoamine oxidase-A expression in high grade prostate cancer. J. Urol. 180 (2008) 2206–2211. DOI: 10.1016/j.juro.2008.07.019

25. C.P. Liao, T.P. Lin, P.C. Li, L.A. Geary, K. Chen, V.P. Vaikari, J.B. Wu, C.H. Lin, M.E. Gross, J.C. Shih. Loss of MAOA in epithelia inhibits adenocarcinoma development, cell proliferation and cancer stem cells in prostate. Oncogene 37 (2018) 5175–5190. DOI: 10.1038/s41388-018-0325-x

26. X. Wu, J. Wu, J. Huang, W.C. Powell, J. Zhang, R.J. Matusik, F.O. Sangiorgi, R.E. Maxson, H.M. Sucov, P. Roy-Burman. Generation of a prostate epithelial cell-specific Cre transgenic mouse model for tissue-specific gene ablation. Mech. Dev. 101 (2001) 61–69. DOI: 10.1016/s0925-4773(00)00551-7

27. S. Wang, J. Gao, Q. Lei, N. Rozengurt, C. Pritchard, J. Jiao, G.V. Thomas, G. Li, P. Roy-Burman, P.S. Nelson, X. Liu, H. Wu. Prostate-specific deletion of the murine Pten tumor

suppressor gene leads to metastatic prostate cancer. Cancer Cell 4 (2003) 209–221. DOI: 10.1016/s1535-6108(03)00215-0

28. K. Chen, D.P. Holschneider, W. Wu, I. Rebrin, J.C. Shih. A spontaneous point mutation produces monoamine oxidase A/B knock-out mice with greatly elevated monoamines and anxiety-like behavior. J. Biol. Chem. 279 (2004) 39645–39652. DOI: 10.1074/jbc.M405550200

29. R.M. Bingisser, P.A. Tilbrook, P.G. Holt, U.R. Kees. Macrophage-derived nitric oxide regulates T cell activation via reversible disruption of the Jak3/STAT5 signaling pathway. J. Immunol. 160 (1998) 5729-5734.

30. A.E. Ryan, A. Colleran, A. O'Gorman, L. O'Flynn, J. Pindjacova, P. Lohan, G. O'Malley, M. Nosov, C. Mureau, L.J. Egan. Targeting colon cancer cell NF-kappaB promotes an anti-tumour M1-like macrophage phenotype and inhibits peritoneal metastasis. Oncogene 34 (2015) 1563-1574. DOI: 10.1038/onc.2014.86

31. A.L. Doedens, C. Stockmann, M.P. Rubinstein, D. Liao, N. Zhang, D.G. DeNardo, L. MCoussens, M. Karin, A.W. Goldrath, R.S. Johnson. Macrophage expression of hypoxia-inducible factor-1 alpha suppresses T-cell function and promotes tumor progression. Cancer Res. 70 (2010) 7465-7475. DOI: 10.1158/0008-5472.CAN-10-1439

32. N. Takeda, E.L. O'Dea, A. Doedens, J. Kim, A. Weidemann, C. Stockmann, M. Asagiri, M.C. Simon, A. Hoffmann, R.S. Johnson. Differential activation and antagonistic function of HIF-{alpha} isoforms in macrophages are essential for NO homeostasis. Genes Dev. 24 (2010) 491-501. DOI: 10.1101/gad.1881410

33. S. Davidsson, A.L. Ohlson, S.O. Andersson, K. Fall, A. Meisner, M. Fiorentino, O. Andrén, J.R. Rider. CD4 helper T cells, CD8 cytotoxic T cells, and FOXP3(+) regulatory T cells with

respect to lethal prostate cancer. Mod. Pathol. 26 (2013) 448-455. DOI: 10.1038/modpathol.2012.164

34. J.M. Austyn, S. Gordon. F4/80, a monoclonal antibody directed specifically against the mouse macrophage. Eur. J. Immunol. 11 (1981) 805-815. DOI: 10.1002/eji.1830111013

35. A.J. Garcia, M. Ruscetti, T.L. Arenzana, L.M. Tran, D. Bianci-Frias, E. Sybert, S.J. Priceman, L. Wu, P.S. Nelson, S.T. Smale, H. Wu. Pten null prostate epithelium promotes localized myeloid-derived suppressor cell expansion and immune suppression during tumor initiation and progression. Mol. Cell Biol. 34 (2014) 2017-2028. DOI: 10.1128/MCB.00090-14

36. H. Mizoguchi, J.J. O'Shea, D.L. Longo, C.M. Loeffler, D.W. McVicar, A.C. Ochoa. Alterations in signal transduction molecules in T lymphocytes from tumor-bearing mice. Science 258 (1992) 1795-1798. DOI: 10.1126/science.1465616

37. H. Ikeda, L.J. Old, R.D. Schreiber. The roles of IFN gamma in protection against tumor development and cancer immunoediting. Cytokine Growth Factor Rev. 13 (2002) 95-109. DOI: 10.1016/s1359-6101(01)00038-7

38. M. Kubera, M. Maes, G. Kenis, Y.K. Kim, W. Lasoń. Effects of serotonin and serotonergic agonists and antagonists on the production of tumor necrosis factor alpha and interleukin-6. Psychiatry Res. 134 (2005) 251-258. DOI: 10.1016/j.psychres.2004.01.014